Autophagy flux modulates Tax viral protein distribution pattern in human T-cell lymphotropic virus type 1 (HTLV-1) infection

Nicolás Ducasa
Instituto de investigaciones biomédicas en retrovirus y SIDA (INBIRS) https://orcid.org/0000-0003-4455-8295
Daniel Grasso
Instituto de Estudios de la Inmunidad Humoral (IDEHU)
Paula Benencio
Instituto de investigaciones biomédicas en retrovirus y SIDA (INBIRS)
Daniela Papademetrio
Instituto de Estudios de la Inmunidad Humoral (IDEHU)
Mirna Biglione
Instituto de investigaciones en retrovirus y SIDA (INBIRS)
Fatah Kashanchi
Laboratory of Molecular Virology
Maria Noe Garcia
Instituto de Estudios de la Inmunidad Humoral (IDEHU)
Carolina Berini (caroberini@gmail.com)
CONICET- Universidad de Buenos Aires

Research

Keywords: Autophagy, HTLV-1, TAX, LC3

Posted Date: May 28th, 2020

DOI: https://doi.org/10.21203/rs.3.rs-30628/v1

Abstract

Background

Viruses can evade the host's immune response promoting their survival and proliferation by different mechanisms. It has recently been observed that viruses can also manipulate autophagy mechanism/pathway for their own benefit. Autophagy is a conserved catabolic process for intracellular components, such as proteins and organelles, and it is important in maintaining cellular homeostasis. Human T-cell lymphotropic virus type 1 (HTLV-1) is the causative agent of HTLV-1 associated Myelopathy/ Tropical Spastic Paraparesis (HAM/TSP), Adult T-cell Leukemia/Lymphoma (ATLL) and Bronchiectasis. HTLV-1 has been reported to regulate autophagy favoring viral production. Viral protein Tax blocks the fusion of the autophagosome with the lysosome, preventing degradation and increasing the accumulation of autophagosomes. Yet, the role of autophagy in HTLV-1 infection has not been fully described. The aim of this study was to determine if the autophagic state conditions regulate HTLV-1 infection.

Results

Tax was distributed in specific patterns and spherical structures in infected Jurkat, HeLa and MT2 cell lines. Autophagic flux treatments modified Tax behavior in infected HeLa and MT2 cell lines as analyzed by confocal microscopy and flow cytometry, respectively. Utilizing relative quantification of mRNA by qPCR, the variation of other viral genes was analyzed, observing a similar pattern for each treatment.

Conclusions

These results provide evidence that the autophagic state is shown to control HTLV-1 infection. In addition, Tax can be observed in spherical structures linked to the plasma membrane which could be involved in promoting viral propagation. By carrying out this research, we hope to elucidate fundamental mechanisms for the propagation of HTLV-1 that would involve the use of the autophagic pathway, providing a potential therapeutic target to prevent the development of pathologies associated with HTLV-1 infection.

Background

Human T-cell lymphotropic viruses (HTLVs) are retroviruses that infect approximately 15–25 million people worldwide [1]. HTLV-1 infection is associated with several severe pathologies, mainly a neurological disease called HTLV-1 Associated Myelopathy or Tropical Spastic Paraparesis (HAM/TSP), a hematologic disease called Adult T-cell Leukemia/ Lymphoma (ATLL), and an immune-deficient state resulting in bronchiectasis [2, 3]. There are no effective treatments for any of their associated pathologies. It is estimated that 5% of people infected with HTLV-1 will develop one of the associated

pathologies [4]. Diseases associated with HTLV-1 infection are characterized by profound dysregulation of CD4 + T cells in terms of activation, immune function, and apoptosis, all of which are facilitated by the pleiotropic functions of the viral oncoprotein Tax [5, 6].

Autophagy is one of the main pathways of macromolecule degradation, key in the recycling of proteins, RNA and other cytoplasmic macromolecules, including whole organelles [7]. The nutritional and metabolic state of cells is sensed by the mechanistic target of rapamycin complex 1 (mTORC1), a negative regulator of autophagy, which detects the decrease in nutrients and growth factors availability as well as stress, allowing to regulate the autophagy process to preserve cellular homoeostasis [8]. Under unfavorable conditions, mTORC1 is inhibited, resulting in the activation of the unc-51 Like Autophagy Activating Kinase 1 (ULK1) complex that activates Beclin 1, in a complex with PI3P kinase activity, which promotes the generation of phosphatidylinositol 3-phosphate (PI3-P) which is vital to the formation of the initial phagophore structure and initiates the nucleation stage [9]. Local production of PI3P leads to the growth of the omegasome and the formation of the isolation membrane that expands, sequestering cytosolic proteins, aggregates and organelles until it matures and closes. Evolutionarily-conserved genes called autophagy related genes (ATG) participate in the formation of the double-membrane vesicles, called autophagosomes, which ends when they incorporate microtubule-associated protein 1A/1B-light chain 3 (LC3-II) into the membrane. The autophagosome eventually fuses with a lysosome (autolysosome) where the sequestered material is degraded and recycled in the cytosol [10, 11].

Autophagy can take an antiviral or proviral role. It could degrade intracellular pathogens, but certain viruses have evolved to use the autophagic machinery for their own benefit, increasing viral replication and viral spread [12].

HTLV-1 Tax viral protein directly inhibits apoptosis and regulates the cell cycle by interacting with the cAMP response element-binding protein (CREB) [13]. It promotes transcriptional activation through CBP/p300 and regulates several signaling pathways, such as the IκB kinase (IKK)/ nuclear factor-kappa B (NF-κB), DNA damage response, and innate immunity [14, 15]. HTLV-1 has been reported to increase the accumulation of autophagosomes, favoring viral production. Tax blocks the fusion of the autophagosome with the lysosome, preventing degradation and an increase in the accumulation of autophagosomes. Furthermore, it was observed that Bafilomycin A, an inhibitor of the fusion of the autophagosome with the lysosome, increased Tax expression [16]. It was observed that Tax maintained the NF-κB signaling pathway active by stimulation of the IKK complex. The autophagic protein Beclin 1 is essential for the maintenance of this activation interacting with the IKK complex. In Beclin 1 depleted cells, Tax was unable to activate NF-κB and signal transducer and activator of transcription 3 (STAT3) to their full capacity and reduced the viability of HTLV-1-transformed T cells [17]. At the same time, Tax has been shown to deregulate autophagy by recruiting the autophagic proteins Beclin 1 and Bif-1 to lipid raft domains (LRD) on the plasma membrane which was dependent on the interaction of Tax with the IKK complex. Collectively, this evidence shows that Tax plays a critical role in autophagy dysregulation, which has an impact on promoting survival and transformation of virally infected T cells [18, 19]. The aim of this study was to determine if the autophagic state regulates HTLV-1 infection.

Methods

Cell line cultures

HeLa cells were cultured in Dulbecco's Modified Eagle Medium (DMEM; Hyclone, Logan, United States) supplemented with 10% fetal bovine serum (Sigma Aldrich, Saint Louis, United States), L-glutamine (2mM/L) and streptomycin (100 µg/ml), at 37° C in 5% CO_2. MT2 cells (persistently infected with HTLV-1) and Jurkat cells infected with HTLV-1 were grown in Roswell Park Memorial Institute 1640 (RPMI) medium (Gibco, Waltham, United States) supplemented with 10% fetal bovine serum, L-glutamine (2mM/L) and streptomycin (100 µg/ml), at 37° C in 5% CO_2. As for the different treatments regarding the autophagic flux, for starvation experiments, cells were incubated in Earle's balanced salts solution (EBSS – Gibco); Spautin-1 10 µM (SP-1 – Sigma) and Chloroquine 100 µM (CQ – Sigma) were used as early and late autophagy flux inhibitors, respectively.

Infection of HeLa cells by co-culture with MT2

Infection of HeLa cells by HTLV-1 was performed by co-culture with MT2 cells. Prior to co-culture, MT2 cells were lethally irradiated at 60 Gy (6000 rads) and washed three times with 1x saline phosphate buffer (PBS 1x). HeLa cells ($2x10^6$) were cultured in a T75 flask at 30% confluence and MT2 irradiated cells ($9x10^6$) were added to the co-culture in 15 ml of DMEM with 10% fetal bovine serum, at 37 °C in 5% CO_2. The co-culture was maintained for three days until HeLa cells reached confluency and reached the number of MT2 cells used (1: 1 ratio). HeLa and MT2 cells were cultured alone as controls.

Determination of the efficiency of infection by flow cytometry

The efficiency of infection of HeLa cells was determined by flow cytometry. To reveal HeLa infected cells, the viral protein Tax was labelled with Anti-Tax-Dyelight 688 antibodies (kindly provided by Dr. Tanaka of the University of Ryukyus, Japan). CD4 was labeled with anti-CD4-PercP (BD, San Jose, United States) to differentiate MT2 cells from HeLa cells. cells ($1x10^5$) were used for each condition. For intracellular labelling, cells were washed with 1 ml of PBS 1x AA (Azide/Albumin, 1000 ml of PBS 1x + 1 gr Albumin + 2 ml Azide 10%). Then the cells were treated using the commercial fixation and permeabilization solution kit (BD Cytofix/Cytoperm, San Jose, United States) according to the manufacturer's instructions. The antibodies were incubated for 40 minutes at 4°C in the dark. After incubation, the cells were resuspended in 100 µl of PBS 1x AA and analyzed by flow cytometry (BD FACS CANTO I, BD Biosciences, San Jose, United States). Data were analyzed using BD FACS Diva (BD Biosciences, San Jose, United States) and FlowJo (BD, San Jose, United States) software's. A corresponding isotype control was used in each case.

Determination of infection by Western Blot

The Western Blot technique was performed to verify the infection of HeLa cells in co-culture where non-infected cells were used as controls. Five milliliter cultures were transferred to a pre-cooled 15 ml conical tube (infected and non-infected conditions), placed on ice and washed with 1x PBS at 4°C. After lysis

with RIPA buffer, tubes were centrifuged at 14,000 rpm for 10 minutes at 4 ° C. The tubes were placed on ice and the supernatant was transferred to new tubes. Each lysate (15 µl) were taken for protein quantification (BCA protein Assay Kit) and Laemmli 4X buffer was added to the remaining material. Proteins (70 µg) were separated in 15% sodium dodecyl sulfate polyacrylamide gel electrophoresis (SDS-PAGE), together with the molecular weight marker. The antibodies used included a 1:700 dilution of primary rabbit antibody anti-Tubulin (eBioscience, San Diego, United States), a 1:500 dilution of primary mouse antibody anti-Tax (Abcam, Cambridge, United Kingdom), a 1:5000 dilution of anti-rabbit-HRP (Santa Cruz, Dallas, United States) and a dilution 1:5000 anti-mouse-HRP (Santa Cruz, Dallas, United States).

Indirect immunofluorescence of Tax and LC3-II

In HeLa cells infected with HTLV-1, treatments on the autophagic flux were performed. The treatments used were starvation, CQ, starvation with CQ and SP-1. All treatments were performed at 2 h, except for SP-1 treatment that was performed at 12 h. SP-1 inhibits the activity of two ubiquitin-specific peptidases causing an increase in proteasomal degradation, which have been shown to regulate autophagy, and therefore longer incubation times are needed. Indirect immunofluorescence was performed from the treated cells. Tax and LC3-II proteins were labeled in infected and uninfected HeLa cells. Cells were fixed with chilled 4% paraformaldehyde for 10 minutes at room temperature and treated with permeabilization solution (PBS 1x + 0.05% X-100 triton) for 10 minutes. Then, the cells were incubated for 1 h at room temperature with blocking solution (PBS 1x + 10% fetal bovine serum). In each step it was washed with PBS 1x. The cells were incubated with a 1:500 dilution of primary mouse antibody anti-Tax (Abcam, Cambridge, United Kingdom) and 1:500 primary rabbit antibody anti-LC3-II (Cell Signaling, Danvers, United States) for 12 h at 4° C. It was washed three times with PBS 1x and the cells were incubated with the conjugated secondary antibodies, anti-mouse Alexa 488 and anti-rabbit Alexa 647 in a 1:700 dilution for 2 h. Finally, they were incubated with Hoechst (Thermofisher, Waltham, United States) for 15 minutes to label nucleic acids and mounted with polyvinyl acetate (PVA). This protocol was also used to observe the distribution of Tax and LC3-II in HTLV-1 infected Jurkat cells and persistently HTLV-1 infected MT2 cells. Unlabeled cells were used as control to establish autofluorescence in each case. Images were acquired with a Carl Zeiss LSM 800 spectral confocal microscope. The processing, analysis and quantification of the images were carried out with the FIJI software.

Relative quantification of HTLV-1 mRNA expression by qPCR from treatments on autophagic flux

In the MT2 cell line, treatments on the autophagic flux were performed to quantify the relative expression of HTLV-1 mRNA. The treatments used were starvation, chloroquine, starvation with chloroquine and SP-1. All treatments were performed at 1 h, 2 h and 3 h, except for SP-1 treatment that was performed at 12 h. Total RNA was isolated by using TRIzol (Invitrogen). Total samples were treated with RQ1 RNase-Free DNase (Promega) and 1 µg of total RNA were reverse-transcribed into complementary DNA by using a MMLV (Promega) according to the manufacturer's instructions. *Pol*, *tax* and *p19* mRNA expression was

measured by qPCR with Eva green reagents (Solis BioDyne) and GAPDH gene expression was used as an internal control. The expression of the viral genes was normalized to GAPDH by using the ($2^{-\Delta\Delta Ct}$) ratio.

Mean fluorescent intensity (MFI) of Tax after treatments on autophagic flux

In the MT2 cell line, expression levels of Tax viral protein were assayed in function of treatments on the autophagic flux. Cells were subjected to starvation, chloroquine and the combination of both for 2 h. For intracellular labelling, cells were washed with 1 ml of PBS 1x AA (Azide/Albumine, 1000 ml of PBS 1x + 1g Albumin + 2 ml Azide 10%). Then the cells were treated using the commercial fixation and permeabilization solution kit (BD Cytofix/Cytoperm, San Jose, United States) according to the manufacturer's instructions. The cells were incubated with a 1:500 dilution of primary mouse antibody anti-Tax (Abcam, Cambridge, United Kingdom) for 5 h at 4°C in darkness. Then it was incubated with a 1:700 the secondary antibody anti-mouse (Alexa 488) for 2 h at 4°C in the darkness. After incubation, the cells were resuspended in 100 µl PBS AA 1x and analyzed by flow cytometry (BD FACS CANTO I, BD Biosciences, San Jose, United States). The results were analyzed using BD FACS Diva (BD Biosciences, San Jose, United States) and FlowJo (BD, San Jose, United States) software. The corresponding isotype control was used in each case.

Statistics

To study the significance between groups, a one-way ANOVA was used. Values were expressed as mean ± SEM. All significance tests were 2-tailed, and the level of significance was set at 0.05. All cell lines data shown are representative of at least 5 independent experiments. Statistical tests were performed with the SPSS 21 program.

Results

MT2-mediated HTLV-1 infection of HeLa cells

With the objective of demonstrating that HeLa cells can be effectively infected with HTLV-1 virus, a co-culture of these cells with the constitutively infected T cell leukemia derived MT2 line was performed. Afterwards, CD4 and the Tax viral protein expressions were analyzed by flow cytometry separately for each cell line post-co-culture. According to the morphological analysis of HeLa cells by flow cytometry, we observed that they had a size distribution between 120 and 240 K, with a membrane complexity between 20 and 100 K. On the other hand, we observed that MT2 cells were comparatively smaller with a size distribution between 80 and 200K, and with a membrane complexity between 20 and 80K. Next both cell lines were labelled with anti-CD4 given that CD4 was only present in the MT2 cell line (99.3%). The same was performed with an anti-Tax APC antibody and both, HeLa and the MT2 cell lines, were evaluated. As expected, most MT2 cells were infected with HTLV-1, evidenced by the presence of Tax. Once the CD4 and Tax staining were carried out separately, we proceeded to analyze them in the co-culture essays. Data in (Fig. 1a) shows a density plot in which HeLa cells cannot be distinguished from MT2. However, in (Fig. 1b), the presence of two populations clearly defined by the presence/absence of anti-CD4 labelling are

observed, with HeLa cells being negative for CD4 and MT2 cells positive for presence of CD4. Analyzing specifically the CD4 positive cells, i.e. MT2 cells, it was observed that 93.2% have an anti-Tax signal, confirming the HTLV-1 infection state of these cells. In order to determine the percentage of HeLa cells infected by co-culture, the presence of Tax fluorescent signal in the CD4 negative population was analyzed. Data in (Fig. 1f) show that 8.67% of CD4 negative population, was positive for a Tax signal. To support the above data, a Western Blot technique was used to verify that the HeLa cells were infected with HTLV-1 by co-cultivation with MT2 cells. Western Blot detected the presence of Tax viral protein in lysates from HeLa cells exposed to MT2 cells co-culture and it was absence in the monoculture. Altogether, this data suggests that HeLa cells are susceptible to HTLV-1 infection and indeed they are infected by MT2 cells in co-culture (Fig. 1g).

Tax distributes with a specific pattern in HTLV-1 infected HeLa cells

The distribution pattern of the viral Tax protein in infected HeLa cells was evaluated using immunofluorescence. As it can be observed in (Fig. 1h), MT2-mediated infected HeLa cells possess a diffuse pattern of Tax distribution into the nucleus. Interestingly, Tax signal is also observed in discrete spots throughout the cytoplasm. It is noteworthy to indicate the presence of Tax distribution as defined domains just above the plasma membrane of the HeLa infected cells, as indicated by arrow (Fig. 1h).

Autophagy controls distribution pattern of Tax in infected HeLa cells

Following infection with MT2 cells, HeLa cultures were subjected to different treatments in order to modulate the autophagic pathway and distribution of Tax viral protein and the autophagosomes marker LC3 were evaluated. As expected, starvation induced autophagic flux that is evidenced by the increase in cytoplasmic LC3 puncta dots (Fig. 2b). Moreover, compared to control, starvation also results in a significant increase in size of Tax positive dots (Fig. 2b and f). Importantly, changed in autophagy pathway was observed when using inhibitors. Chloroquine (CQ) is a lysosomotropic agent that prevents lysosome acidification which inhibits lysosomal enzyme and autophagosome-lysosome fusion. Also CQ treatment results in a blockade of the autophagic flux at late steps which can be observed by the increased presence, due to accumulation, of LC3 positive autophagosomes (Fig. 2c). CQ treatment did not show a modification in Tax signal pattern. However, the combination of induction of autophagy by mean of starvation with a blockade of the same pathway with CQ significantly increase the number of Tax positive spots (Fig. 2d and f). Furthermore, an impairment of autophagy by Spautin-1 (SP-1), which inhibits autophagosome biogenesis, also increased the number of Tax dots in HTLV-1 infected HeLa cells (Fig. 2e and g). Consequently, it is evident that Tax dots redistribute with the modification of autophagy status.

It is interesting to note that the distribution of Tax in the cytoplasm of infected HeLa cells included the presence of numerous domains associated with the plasma membrane of the cells (Fig. 3). Altogether, data suggest that the HTLV-1, or at least the Tax protein, reacts and modifies its behavior in response to autophagy flux state in the infected cell.

Tax is also observed in plasma membrane of MT2 cells persistently infected with HTLV-1

Having observed the presence of Tax in the plasma membrane of infected HeLa cells and considering the previously published data localizing placing Tax in the LRDs of the plasma membrane [18,19], it was important to know whether such observation could be detected in MT2 cells. As it is depicted in Fig. 4, Tax was found in discrete domains of the plasma membrane in MT2 cells. Surprisingly, Tax colocalizes with the autophagy marker LC3 in the same region.

Tax pattern in HTLV-1 infected Jurkat cells

Finally, we use the Jurkat lymphoid cell line to analyze HTLV-1 infection. An important expression, in discrete domains, of Tax in the cytoplasm of infected cells is observed by immunofluorescence (Fig. 5a). Much of the Tax signal was found as domains associated with the plasma membrane (Fig. 5b and c). It is interesting note the observation of macromolecular spherical structures in which Tax signal was localized as part of the external borders in puncta pattern (Fig. 5b and c). Moreover, Tax cytoplasmic signal had a partial colocalization with the autophagic LC3 protein (Fig. 5d). Paying particular attention to the structures formed by Tax in Jurkat cells that can be seen in Fig. 5c, we decided to do a Z scan to better localize the Tax protein. Data in Fig. 5e show that the scan on the Z axis confirmed spherical structures, where Tax domains were located at their edges and with certain regions colocalizing with LC3. We observed that Tax formed spherical structures in a pattern of domains of the structure's boundaries.

Quantification of HTLV-1 genes expression by qPCR

Treatments on the autophagic flux (i.e. starvation, chloroquine, starvation with chloroquine and spautin-1) were performed in MT2 cell lines at 1 h, 2 h and 3 h, except for SP-1 treatment that was performed at 12 h. Data in Fig. 6a show the relative expression of viral protein Tax, p19 and Pol under each condition after 1 h of treatment. We observed that the starvation and CQ alone treatments enhanced the expression of both p19 and Pol. After 2 h post treatment there was an increase of viral gene expression under all conditions (Fig. 6b). After 3 h post-treatment, there was a marked increase in viral gene expression when autophagy was enhanced by starvation and then inhibited with CQ (Fig. 6c). We also observed that the inhibition of autophagy with CQ alone decreased viral expression (Fig. 6c). SP-1 treatment after 12 h showed marked increase in viral gene expression (Fig. 6d) indicating that Tax and other viral proteins increase their expression when autophagy is modulated; in concordance with the results obtained in confocal microscopy.

Changes in mean fluorescent intensity of Tax after treatments on autophagic flux

Next starvation, CQ and a combination of both were applied to MT2 cells for 2 h. Fig. 6e shows the Mean fluorescent intensity (MFI) measurements of Tax expression by flow cytometry. We observed that under the treatments that modify autophagy flux, Tax behaves in a similar manner as observed previously. The expression of Tax was modified by the condition of the autophagic flux. This increase in viral expression suggests the influence of the autophagic state.

Discussion

Regarding the study of autophagy in HTLV-1 infection, we decided to start this analysis using HeLa cell line since it is the most utilized and standardized model for the study of autophagy machinery [18, 19]. In this sense, it was possible to set up a method of infection by co-culture of HeLa cells with persistently infected MT2 cells [16]. The methodology used allowed us to obtain cultures with acceptable infection percentages for subsequent studies. It was possible to consistently differentiate each cell population in the co-culture by flow cytometry. The specific immunofluorescence for Tax showed that in infected HeLa cells this viral protein had an important diffuse pattern in the nucleus. In the cytoplasm, it is interesting to note that Tax presented, unlike the nucleus, a pattern focused on well-defined domains throughout the cell and associated with the plasma membrane.

The modulation of the autophagic flux by means of different treatments caused significant changes in the behavior of Tax. Nutrient deprivation, a physiological inducer of autophagy, in HeLa cells caused a significant increase in the average size of the positive domains for Tax. Tax-positive domains could be comprised by multiprotein complexes forming macromolecular structures, nucleation of factors that make the viral cycle or even some type of vesicle, including multivesicular bodies or autophagosomes although the resolution of such question will remain open ended for further studies. These results are in accordance to previous studies in which it was demonstrated that Tax inhibited the fusion of the autophagosome with the lysosome, promoting the accumulation of autophagosomes within the cell [16]. Regardless of the nature of Tax cytoplasmic signal, it is evident that it reacted to the change in the nutritional status of the cell culture. Nutrients deprivation is a very limiting situation for the maintenance of cell homeostasis producing cell changes in the host, so the use of specific autophagic flux inhibitors may better reflect the relationship between this pathway and HTLV-1 infection. It is interesting to note that both, a specific inhibitor of the first steps of the biogenesis of autophagosomes, SP-1, and the inhibition of autophagosome-lysosome fusion at the end of the fasting autophagic pathway, produced a significant increase in the number of Tax fluorescent domains in infected cells. This confirms that the behavior of Tax protein is altered and conditioned by the state of autophagy. Previous studies demonstrated that Tax stimulated the activity of the pro-autophagic protein Beclin 1 by constantly activating the IKK complex and, in turn, NF-κB which promotes the formation of autophagosomes on lipid raft microdomains in the plasma membrane, as seen in Fig. 1c where Tax localizes in the plasma membrane potentially inducing autophagy from these sites [17–19]. Whether this increase is due to a net increase of these structures in the cytoplasm or the inhibition of Tax output from the cell, still requires future investigations. The latter could be in line with the results presented in Fig. 1, where the modification of starvation and/or chloroquine, autophagy seems to increase the amount of Tax associated to the plasma membrane.

Considering these results, we also looked into Tax localization in MT2 cells. Here, we observed that Tax was also present on the plasma membrane. What is also interesting, is that the discrete domains of Tax in the plasma membrane colocalized with the autophagosome marker LC3. Taking into account the previous findings of the recruitment of Beclin 1 (a key autophagy protein) to LRD [18, 19], our results suggest the possibility that Tax is capable of triggering autophagy in various cellular regions. Finally,

since the natural target of HTLV-1 is lymphoid cells, we repeated the experiments on the Jurkat lymphoid cell line. HTLV-1 MT2-mediated infection in Jurkat cells demonstrated similar results to that observed in HeLa cells, however with partial colocalization of Tax with LC3. Interestingly, in this cell line we observed that Tax also forms comparatively large, spherical structures, often associated to the plasma membrane and where Tax formed very defined domains over the entire spheroid surface. Collectively, our data point to a novel function of Tax where stress conditions that induce autophagy relocates Tax (and possibly other viral proteins) for potential survival of infected cells over a longer period of time contributing to cancer development.

Conclusions

It was observed that autophagy conditions the distribution of HTLV-1 Tax protein, showing a specific localization in spheroid structure domains in the cell cytoplasm and in domains in the cell plasma membrane, when autophagy is induced. Further studies should be carried out in order to elucidate the implications of these results.

Abbreviations

ATG
autophagy related genes
ATLL
adult T-cell Leukemia/Lymphoma
CQ
chloroquine
CREB
cAMP response element-binding protein
DMEM
Dulbecco's Modified Eagle Medium
EBSS
Earle's balanced salts solution
HAM/TSP
HTLV-1 Associated Myelopathy/Tropical Spastic Paraparesis
HTLV
human T-cell lymphotropic virus
IKK
IκB kinase
LC3
microtubule-associated protein 1A/1B-light chain 3
LRD
lipid raft domains

MTORC1
mechanistic target of rapamycin complex 1
NF-κB
nuclear factor-kappa B
PBS
saline phosphate buffer
PI3P
phosphatidylinositol 3-phosphate
PVA
polyvinyl acetate
RPMI
Roswell Park Memorial Institute 1640
SDS-PAGE
sodium dodecyl sulfate polyacrylamide gel electrophoresis
SP-1
spautin-1
STAT3
signal transducer and activator of transcription 3
ULK1
unc-51 Like Autophagy Activating Kinase 1

Declarations

Ethics approval and consent to participate: Not applicable.

Consent for publication: Not applicable.

Availability of data and materials: the datasets used and/or analyzed during the current study are available from the corresponding author on reasonable request.

Competing interests: The authors declare that they have no competing interests.

Funding: The authors are grateful for the funding support by the National Scientific and Technical Research Council (CONICET) and National Agency for Scientific and Technical Promotion (ANPCyT: PICT 2016-1033 CAB, PICT 2016-1105 MNG and PICT 2015-0405 DG).

Authors' contributions: ND performed the experiments, analyzed, interpreted the data and was a major contributor in writing the manuscript. DG was part of the conceptualization, data curation, and methodology design. He has also reviewed and edited the manuscript. PB: helped with the flow cytometry experiments and analyzed the results. DP supervised and discussed the methodology. MB validated the results. FK supervised and discussed the methodology and results. He has also helped with the revision and editing. MNG was part of the conceptualization, helped with funding acquisition, supervised the

methodology, reviewed and edited the manuscript. CB was part of the conceptualization, funding acquisition, supervision and writing of the final manuscript.

Acknowledgements: We gratefully acknowledge the contribution of those persons who helped us at our institutions: INBIRS and IDEHU. A special thanks to Virginia Polo and Carla Pascuale for their help with the cytometer and microscope, respectively. In addition, we would like to thank BIOARS S.A. for being a support in our daily HTLV research.

References

1. Gessain A, Cassar O. Epidemiological Aspects and World Distribution of HTLV-1 Infection. Front Microbiol. 2012;3:388.
2. Futsch N, Mahieux R, Dutartre H. HTLV-1, the Other Pathogenic Yet Neglected Human Retrovirus: From Transmission to Therapeutic Treatment. Viruses. 2017;10(1).
3. Einsiedel L, Pham H, Wilson K, Walley R, Turpin J, Bangham C, et al. Human T-Lymphotropic Virus type 1c subtype proviral loads, chronic lung disease and survival in a prospective cohort of Indigenous Australians. PLoS Negl Trop Dis. 2018;12(3):e0006281.
4. Tagaya Y, Matsuoka M, Gallo R. 40 years of the human T-cell leukemia virus: past, present, and future. [version 1; peer review: 2 approved]. F1000Res. 2019;8.
5. Romanelli MG, Diani E, Bergamo E, Casoli C, Ciminale V, Bex F, et al. Highlights on distinctive structural and functional properties of HTLV Tax proteins. Front Microbiol. 2013;4:271.
6. Fochi S, Mutascio S, Bertazzoni U, Zipeto D, Romanelli MG. HTLV Deregulation of the NF-κB Pathway: An Update on Tax and Antisense Proteins Role. Front Microbiol. 2018;9:285.
7. Mizushima N, Levine B, Cuervo AM, Klionsky DJ. Autophagy fights disease through cellular self-digestion. Nature. 2008;451(7182):1069–1075.
8. Rabanal-Ruiz Y, Otten EG, Korolchuk VI. mTORC1 as the main gateway to autophagy. Essays Biochem. 2017;61(6):565–584.
9. Corona Velazquez AF, Jackson WT. So many roads: the multifaceted regulation of autophagy induction. Mol Cell Biol. 2018;38(21).
10. Dunn WA. Studies on the mechanisms of autophagy: maturation of the autophagic vacuole. J Cell Biol. 1990;110(6):1935–1945.
11. Parzych KR, Klionsky DJ. An overview of autophagy: morphology, mechanism, and regulation. Antioxid Redox Signal. 2014;20(3):460–473.
12. Kudchodkar SB, Levine B. Viruses and autophagy. Rev Med Virol. 2009;19(6):359–378.
13. Yin MJ, Paulssen EJ, Seeler JS, Gaynor RB. Protein domains involved in both in vivo and in vitro interactions between human T-cell leukemia virus type I tax and CREB. J Virol. 1995;69(6):3420–3432.

14. Ishikawa H, Barber GN. STING is an endoplasmic reticulum adaptor that facilitates innate immune signalling. Nature. 2008;455(7213):674–678.
15. Kashanchi F, Brady JN. Transcriptional and post-transcriptional gene regulation of HTLV-1. Oncogene. 2005;24(39):5938–5951.
16. Tang S-W, Chen C-Y, Klase Z, Zane L, Jeang K-T. The cellular autophagy pathway modulates human T-cell leukemia virus type 1 replication. J Virol. 2013;87(3):1699–1707.
17. Chen L, Liu D, Zhang Y, Zhang H, Cheng H. The autophagy molecule Beclin 1 maintains persistent activity of NF-κB and Stat3 in HTLV-1-transformed T lymphocytes. Biochem Biophys Res Commun. 2015;465(4):739–745.
18. Ren T, Takahashi Y, Liu X, Loughran TP, Sun SC, Wang HG, et al. HTLV-1 Tax deregulates autophagy by recruiting autophagic molecules into lipid raft microdomains. Oncogene. 2015;34(3):334–345.
19. Huang J, Ren T, Guan H, Jiang Y, Cheng H. HTLV-1 Tax is a critical lipid raft modulator that hijacks IkappaB kinases to the microdomains for persistent activation of NF-kappaB. J Biol Chem. 2009;284(10):6208–6217.

Figures

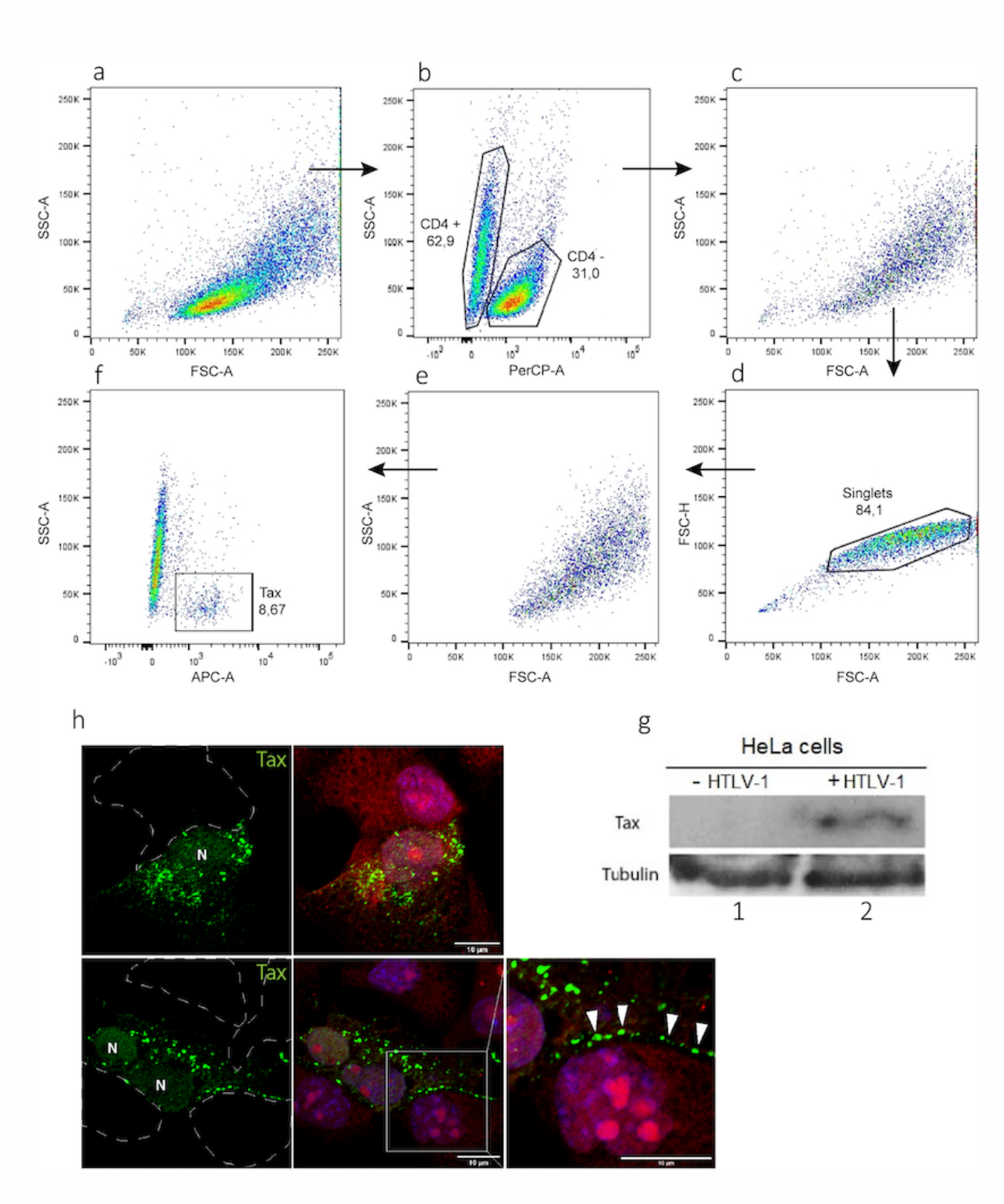

Figure 1

Efficiency of infection and Tax distribution in HTLV-1 infected HeLa by co-cultures with MT2 cells. Flow cytometry gating strategy utilized to analyze the efficiency of HTLV-1 infection in HeLa cells by co-cultivation with MT2 cells. a: analysis of the morphology of the cells in co-culture. b: labelling with anti-CD4 PerCP. c-e: morphology of the negative CD4 population (HeLa cells). f: Percentage of negative CD4 cells that were Tax positive (8.67%). g: Western blot for the viral Tax protein and as a load control the

Tubulin protein, in HeLa cells without having been in co-culture with MT2 cells (1) and HeLa cells after co-culture with MT2 cells (2). h: Tax distribution pattern (green fluorescence) in HeLa cells infected after co-culture with MT2 cells. Diffuse Tax signal is observed in nucleus (N). In cytoplasm Tax is distributed as discrete domains, and a proportion of these are found on the plasma membrane (arrowheads). Autofluorescence in the red channel was used to observe the general morphology of the cells.

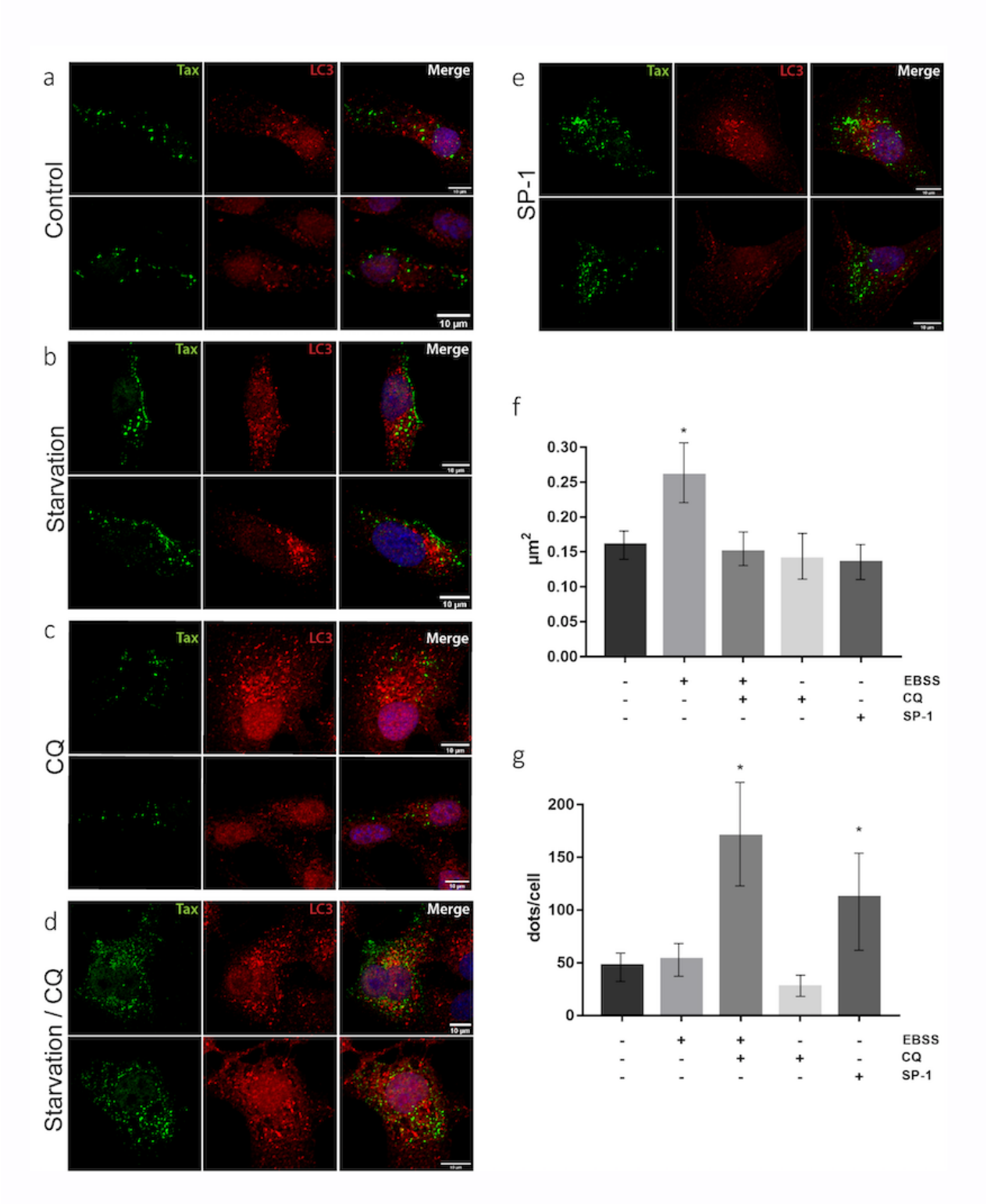

Figure 2

Indirect immunofluorescence under different treatments on the autophagic flux in HeLa cells infected with HTLV-1. a-e: Indirect immunofluorescence against the Tax viral protein (in green) and LC3 (in red) in HeLa cells infected with HTLV-1 and under the indicated treatments. f: Quantification of the size of the cytoplasmic domains of Tax. g: Quantification of the size of the cytoplasmic domains of Tax.

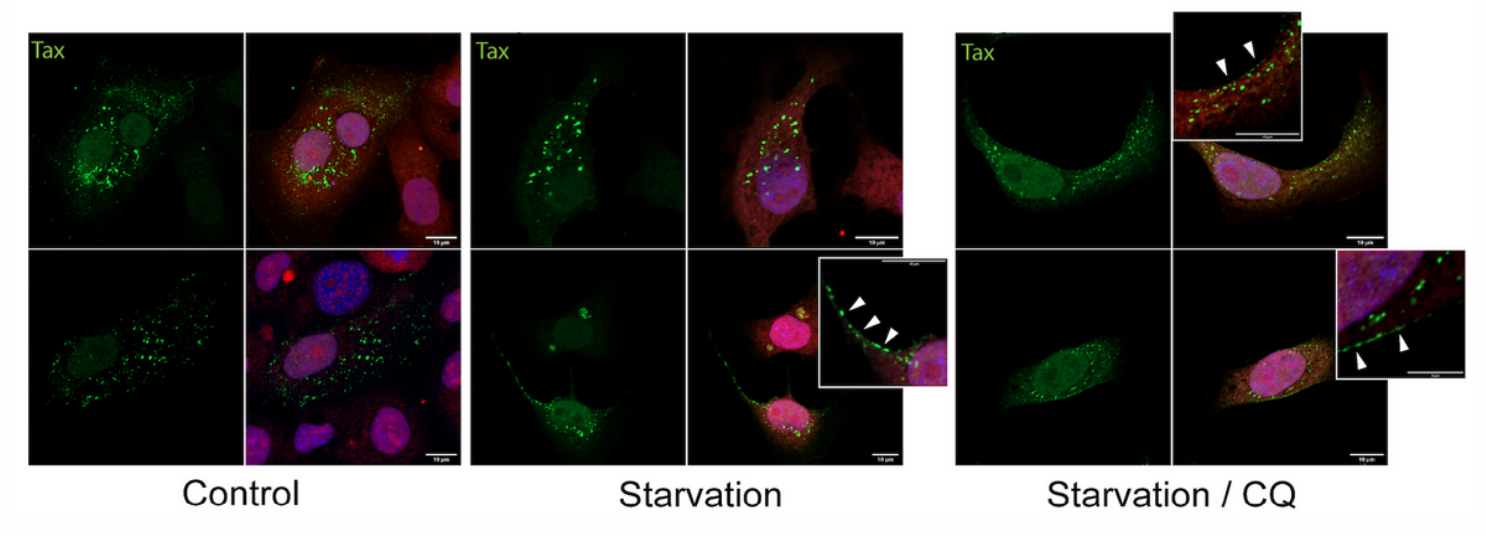

Figure 3

Indirect immunofluorescence of Tax and its distribution after treatments on the autophagic flux. Indirect immunofluorescence of Tax in HeLa cells infected with HTLV-1 and under the indicated treatments. The presence of Tax positive domains associated with the plasma membrane are highlighted (arrowheads). The fluorescence in red is due to the autofluorescence of that channel to observe its morphology.

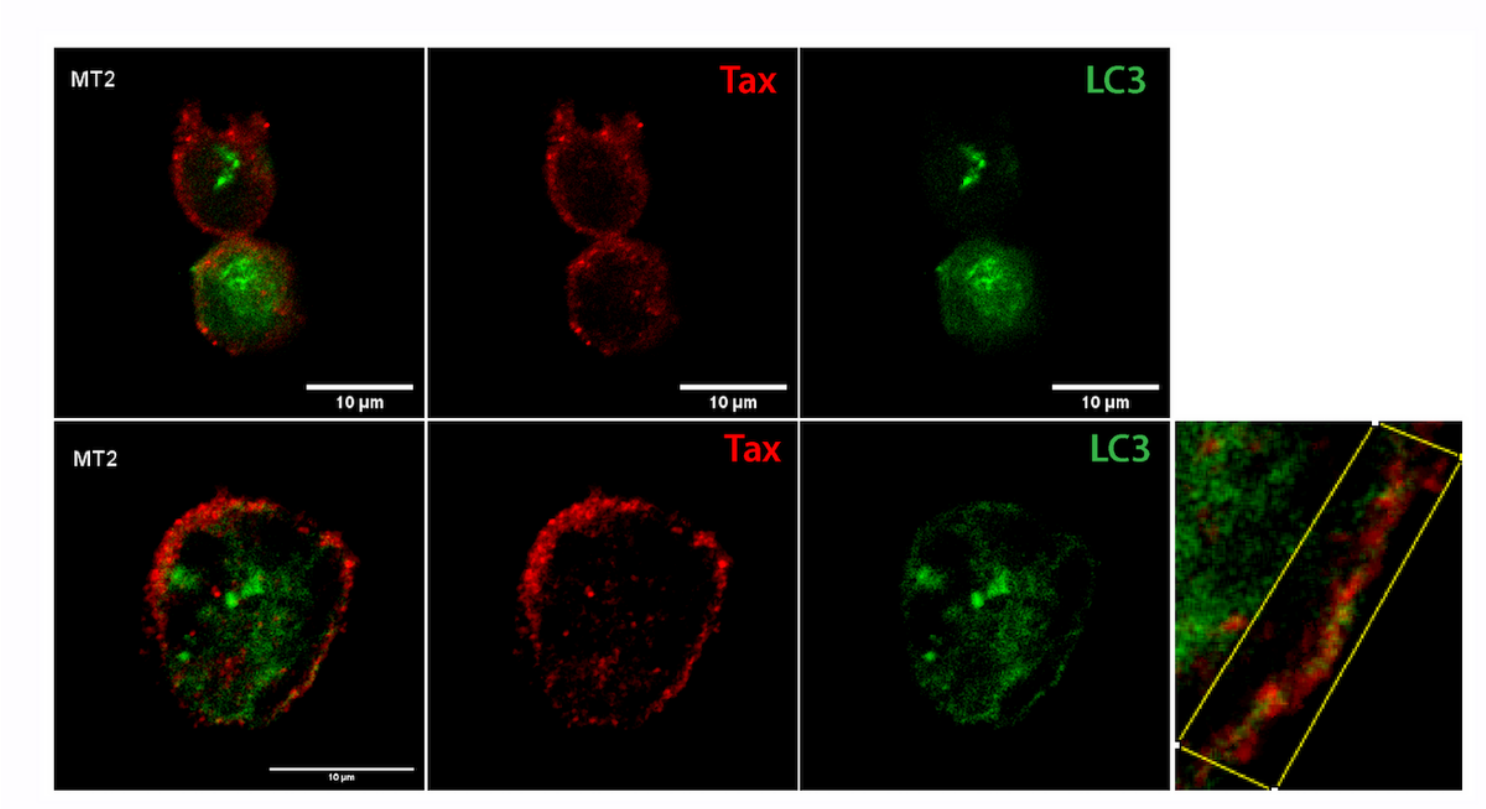

Figure 4

Indirect immunofluorescence of Tax and LC3 in MT2 cells. Indirect immunofluorescence of Tax and LC3 in MT2 cells. Tax and LC3 colocalization is shown in detail (bottom right).

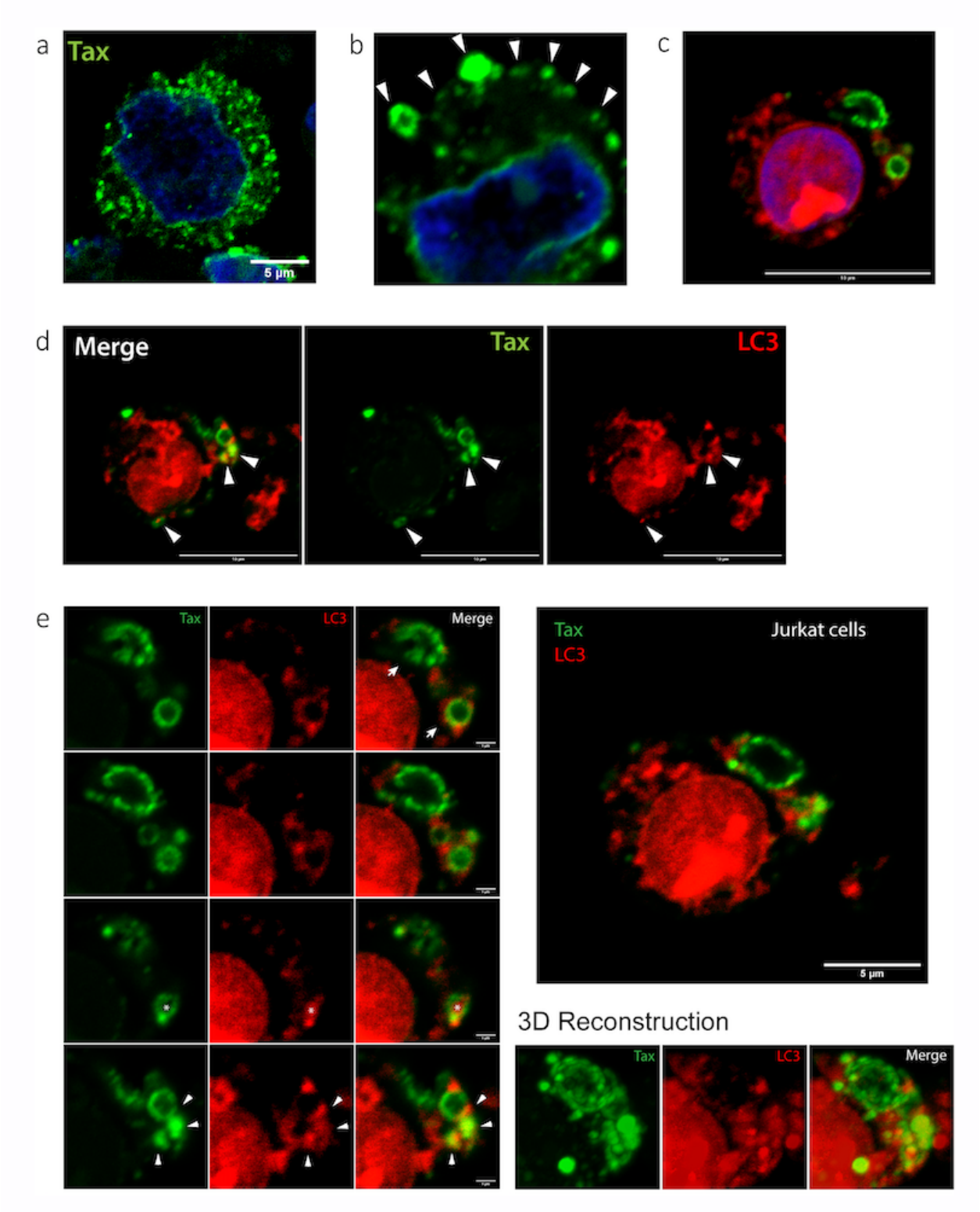

Figure 5

Confocal microscopy and scan on the Z axis of Jurkat cells infected with HTLV-1. a-d: Confocal microscopy of Jurkat cells infected with HTLV-1. Much of the Tax signal was found forming domains and structures of various sizes associated with the plasma membrane. Some Tax-LC3 colocalization points are indicated with arrowheads. e: Confocal scan on the Z axis of Jurkat cells infected with HTLV-1. The different planes in Z are observed with Tax in green mark and LC3 with red. Some Tax-LC3 colocalization points are indicated with arrowheads.

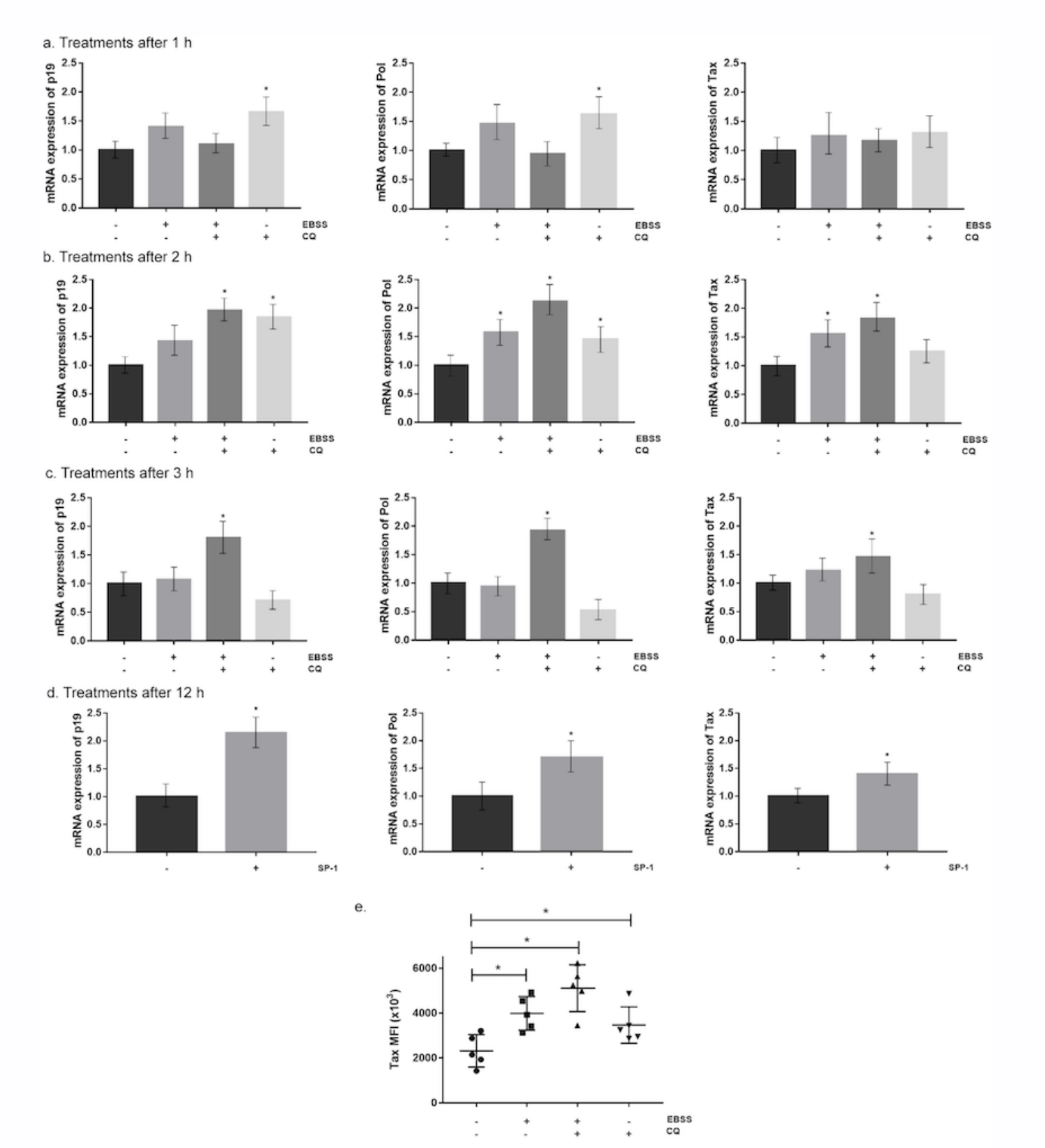

Figure 6

Relative expression of viral genes and Tax expression after treatments on the autophagic flux. Relative expression of tax, p19 and pol mRNA by qPCR after treatments with starvation, chloroquine and starvation with chloroquine. a: Quantification of gene expression after 1 h of treatments. b: Quantification of gene expression after 2 h of treatments. c: Quantification of gene expression after 3 h of treatments. d: Relative expression of tax, p19 and pol mRNA by qPCR after 12 h of treatment with spautin-1. e. MFI levels of Tax after 2 h of starvation, chloroquine and a combination of both.